Supporting Information

Mankowski et al. 10.1073/pnas.1718441115

SI Materials and Methods

Hierarchical Clustering of NAbs. NAbs were grouped into functionally related clusters based upon their neutralization profiles as previously described (1, 2). Neutralization profiles were compared pairwise for all mAbs using Spearman correlation. Spearman rho and *P* values were then used as input for hierarchical clustering as implemented in the "pvclust" package for R (cran.r-project.org/web/packages/pvclust/index.html) (3). This clustering, depicted as a tree, was also used to order a matrix of correlation values produced using the "corrplot" package for R (cran.r-project.org/web/packages/corrplot/index.html) (4).

E1E2 Sequence Analysis. Evolutionary analyses were conducted in MEGA7 (5). Diversity plots were generated using VarPlot v1.2 (6) (https://sray.med.som.jhmi.edu/SCRoftware/VarPlot/) with 1aa steps and 20 aa windows. Inclusion of reference panel polymorphisms in the 11 and 19 HCVpp panels was calculated using a previously described reference alignment from GenBank (7) and the package "seqinr" in R, as previously described (2).

HCVpp Production and Neutralization. HCVpp were produced by lipofectamine-mediated transfection of HCV E1E2, pNL4-3.Luc. R-E-, and pAdVantage (Promega) plasmids into HEK293T cells as previously described (2, 8, 9). Neutralization assays were performed as described previously (10). Single concentrations or serial dilutions of mAbs were incubated with HCVpp for 1 h at 37 °C before addition to Hep3B cells in duplicate. Medium was changed after 5 h, and cells were incubated for 72 h before measurement of luciferase activity in cell lysates in relative light units (RLU). Nonspecific human IgG (Sigma-Aldrich) at the same concentration as the NAbs was used as a negative control. Fraction unaffected (f_u) was calculated by the formula $f_u = \mathrm{RLU}_{\mathrm{mAb}}/\mathrm{RLU}_{\mathrm{nonspecific\ IgG}}$. Fraction affected was calculated by the formula $f_a = 1 - f_u$. Percent neutralization was calculated by the formula percent neutralization $= f_a \times 100\%$. Neutralization by mAb serial dilutions was plotted on median effect plots, with $\log_{10}$[mAb] plotted against $\log_{10}(f_a/f_u)$.

HCVcc Production and Neutralization. Generation of an HCVcc chimera expressing the 1a53 E1E2 proteins was previously described (11, 12). HCVcc neutralization assays were performed in triplicate as previously described (11, 12). Briefly, HCVcc were mixed with serially diluted mAbs, then incubated at 37 °C for 1 h. Medium was removed from the cells and replaced with 50 μL of HCVcc/antibody mixture. Medium was changed after overnight incubation, and cells were incubated for another 48 h at 37 °C. Cells were fixed with 4% formaldehyde, then stained for HCV NS5A using primary anti-NS5A antibody 9E10 (a gift of Charles Rice, The Rockefeller University, New York) at a 1:2,000 dilution, then secondary antibody Alexa Daylight 488-conjugated goat anti-mouse IgG (Life Technologies) at a 1:500 dilution. Images were acquired and spot forming units were counted using an Autoimmun Diagnostika (AID) iSpot Reader Spectrum operating AID ELISpot Reader version 7.0. Percent neutralization was calculated as $100\% \times [1 - (\mathrm{HCVccSFU}_{\mathrm{mAb}}/\mathrm{HCVccSFU}_{\mathrm{nonspecific\ IgG}})]$.

Identification of Synergy/Additivity/Antagonism or Independence Using the Loewe Additivity and Bliss Independence Models. For four selected NAb combinations, two HCVpp were selected for each NAb combination that were at least partially neutralized by 10 μg/mL of each NAb in that combination [$f_u < 0.3$, except HEPC3/1b14 (0.63), HEPC90/1a53 (0.65)]. The combination of HEPC74/HEPC98 was also tested using 1a53 strain HCVcc. Neutralization of HCVpp or HCVcc by serial dilutions of each individual NAb was measured to determine 50% inhibitory concentrations (IC_{50}). Neutralization by serial twofold dilutions of the same NAbs, this time combined in a fixed ratio adjusted for their relative IC_{50}s, was then measured (13). Neutralization by serial dilutions of individual component NAbs was simultaneously measured, using the same antibody concentrations tested in the NAb combination neutralization curve. The f_u and f_a values from the individual NAb neutralization curves were used to calculate neutralization for each NAb combination predicted by the Loewe additivity and the Bliss independence models. Neutralization predicted by the Loewe additivity model was calculated at each antibody concentration using a script in Python (available at https://github.com/mmankowski/Loewe-additivity-calculator) that solves for the first 10 digits of f_{u1+2} in the equation

$$1 = \left[\left(\frac{f_{a_1}}{f_{u_1}}\right)^{1/m_1} \times \left(\frac{f_{u1+2}}{1-f_{u1+2}}\right)^{1/m_1}\right] + \left[\left(\frac{f_{a_2}}{f_{u_2}}\right)^{1/m_2} \times \left(\frac{f_{u1+2}}{1-f_{u1+2}}\right)^{1/m_2}\right],$$

with $f_{u1} = f_u$ of NAb_1, $f_{u2} = f_u$ of NAb_2, m_1 = slope of the median effect plot of NAb_1, and m_2 = slope of the median effect plot of NAb_2; m_1 and m_2 were calculated by linear regression of the median effect plots of component NAb_1 and component NAb_2, respectively, using Prism (Graphpad Software). For each NAb combination, neutralization predicted by the Bliss independence model was calculated at each antibody concentration using the equation

$$f_{u_{1+2}} = f_{u_1} \times f_{u_2}.$$

Loewe additivity-predicted and Bliss independence-predicted neutralization curves were plotted on median effect plots along with the actual experimental NAb combination neutralization curves.

Quality Control for Loewe/Bliss Analysis. NAb combinations were tested in at least two independent experiments against each of two different HCVpp, except HC84.26/HC33.4, which was tested in two experiments against only one strain. Neutralization by individual NAbs and NAb combinations that were compared with each other were measured in the same experiment against the same HCVpp or HCVcc preparation. Only individual NAb curves with linear relationships on median effect plot with *R* squared of >0.85 were used to calculate Loewe additivity and Bliss independence curves (Fig. S5). The means of duplicate points were used to calculate both the *R* squared and *m*. Lines were not required to pass through the point (0,0). To confirm that NAbs were combined in optimal ratios to allow discrimination between Loewe additivity and Bliss independence, predicted Loewe and Bliss curves for each combination were confirmed to be statistically different from each other for at least three antibody concentrations (Fig. S5). NAb concentrations at which either model predicted $f_u < 0.001$ were removed from the experimental vs. Bliss/Loewe comparison, as values this low are outside of the reliable dynamic range of the neutralization assay.

Binding Competition Assays. MAb binding to E1E2 was quantitated using ELISA as previously described (14).[†] Blocking NAbs

[†]Netski DM, et al., 11th International Symposium on Hepatitis C Virus and Related Viruses, October 3–7, 2004, Heidelberg, Germany.

were added first after dilution to either 50 μg/mL (HC84.26, HEPC90/1a142 E1E2) or 20 μg/mL (all other NAbs). Binding NAbs, which had been biotinylated using an EZ-Link NHS-PEG4-Biotin and Labeling Kit (Thermo Fisher Scientific), were added at their EC_{75} (as previously determined using serial dilution binding assays), followed by streptavidin–horseradish peroxidase, and tetramethylbenzidine peroxidase substrate. For HEPC74/HEPC98 binding competition curves, the same protocol was used, but serial fivefold dilutions of both blocking and binding NAb, starting at 50 μg/mL, were used.

Timecourse Inhibition Experiments. Strain 1a154 HCVpp were incubated with HEPC74 at 50 μg/mL or HEPC98 at 5 μg/mL (T-30-min condition), or medium alone for 30 min at 37 °C, chilled to 4 °C, then added to hep3B cells that had been prechilled to 4 °C. For T-30-min condition, CL58 peptide (15), anti-CD81 mAb (BD 555675), anti–SR-B1 mAb (BD 610882), or isotype control mAb (BD 560550) at 50 μg/mL concentration was incubated with hepatoma cells for 30 min, then removed before HCVpp addition. HCVpp were then incubated with cells for 4 h at 4 °C to allow particle attachment without entry. Cells were then washed to remove unattached virus, and cells moved to 37 °C, to allow viral entry. Inhibitors were then added immediately (T0m), after 30 min, 60 min, or 120 min. In each case, inhibitors were incubated with the cells for 30 min total, before washing to remove the inhibitor. Cells were then incubated for 72 h before quantitation of luciferase activity. Percent inhibition was calculated relative to infection of virus absent any inhibitor. Background inhibition was subtracted, and maximal inhibition of each inhibitor was adjusted to 100% to facilitate comparison.

Expression of sE2. A truncated, soluble form of strain 1a154 (H77) E2 ectodomain (sE2), encompassing residues 384 to 645, as previously described (16), was cloned into a mammalian expression vector (phCMV3_Ig Kappa_HIS, a gift of Leopold Kong, The Scripps Research Institute, La Jolla, CA). The sE2 construct was cotransfected with pAdvantage (Promega) into HEK293T cells. Supernatant was collected at 48 and 72 h, passed through a 0.2-μm filter, and concentrated using a regenerated cellulose centrifugal filter with a 10-kDa cutoff (Amicon). Unpurified supernatants were used for heparan binding experiments and ELISA. The sE2 protein used for CHO binding experiments was expressed by transient transfection into HEK293-6E cells. The sE2 was purified from filtered cell supernatants using nickel-nitrilotriacetic acid (GE Healthcare) affinity chromatography and purified further by size exclusion chromatography on a Superdex 200 Increase 10/300 column (GE Healthcare) in 20 mM Tris pH 7.4, 150 mM NaCl.

sE2 Binding to CHO Cells. CHO–CD81 and CHO–SR-B1 binding experiments were carried out as previously described (17, 18). CHO cells expressing recombinant human CD81 or SR-B1 were detached using PBS supplemented with 4 mM EDTA and 10% FBS, incubated with sE2, then 0.5 μg of mouse anti-6x His-tag antibody, then Alexa Fluor 647-labeled goat anti-mouse IgG secondary antibody, then fixed with 1% paraformaldehyde and analyzed on an LSRII cytometer (Becton-Dickinson) using FlowJo software (Tree Star). For mAb binding inhibition experiments, sE2 was preincubated with serial dilutions of mAbs or nonspecific human IgG, then used to stain CHO cells as above.

sE2 Binding to Heparan Sulfate. Heparan binding experiments were carried out essentially as previously described (19). Briefly, strain 1a154 sE2 was incubated with serial dilutions of HEPC74, HEPC98, or nonspecific human IgG, then added to ELISA wells that had been coated with 1 μg of heparan sulfate (Sigma). All proteins were diluted in blocking buffer (0.05% Tween 20, 3% BSA in PBS). The sE2 binding was detected with mouse anti-6x His-tag antibody and goat-anti mouse-HRP antibody (Abcam). Background binding to wells without heparan was subtracted.

1. Bailey JR, et al. (2017) Broadly neutralizing antibodies with few somatic mutations and hepatitis C virus clearance. *JCI Insight* 2:92872.
2. Bailey JR, et al. (2015) Naturally selected hepatitis C virus polymorphisms confer broad neutralizing antibody resistance. *J Clin Invest* 125:437–447.
3. Suzuki R, Shimodaira H (2006) Pvclust: An R package for assessing the uncertainty in hierarchical clustering. *Bioinformatics* 22:1540–1542.
4. Friendly M (2002) Corrgrams: Exploratory displays for correlation matrices. *Am Stat* 56:316–324.
5. Kumar S, Stecher G, Tamura K (2016) MEGA7: Molecular Evolutionary Genetics Analysis version 7.0 for bigger datasets. *Mol Biol Evol* 33:1870–1874.
6. Ray SC, et al. (1999) Acute hepatitis C virus structural gene sequences as predictors of persistent viremia: Hypervariable region 1 as a decoy. *J Virol* 73:2938–2946.
7. Munshaw S, et al. (2012) Computational reconstruction of Bole1a, a representative synthetic hepatitis C virus subtype 1a genome. *J Virol* 86:5915–5921.
8. Hsu M, et al. (2003) Hepatitis C virus glycoproteins mediate pH-dependent cell entry of pseudotyped retroviral particles. *Proc Natl Acad Sci USA* 100:7271–7276.
9. Logvinoff C, et al. (2004) Neutralizing antibody response during acute and chronic hepatitis C virus infection. *Proc Natl Acad Sci USA* 101:10149–10154.
10. Dowd KA, Netski DM, Wang XH, Cox AL, Ray SC (2009) Selection pressure from neutralizing antibodies drives sequence evolution during acute infection with hepatitis C virus. *Gastroenterology* 136:2377–2386.
11. Wasilewski LN, Ray SC, Bailey JR (2016) Hepatitis C virus resistance to broadly neutralizing antibodies measured using replication-competent virus and pseudoparticles. *J Gen Virol* 97:2883–2893.
12. Wasilewski LN, et al. (2016) A hepatitis C virus envelope polymorphism confers resistance to neutralization by polyclonal sera and broadly neutralizing monoclonal antibodies. *J Virol* 90:3773–3782.
13. Chou TC (2006) Theoretical basis, experimental design, and computerized simulation of synergism and antagonism in drug combination studies. *Pharmacol Rev* 58: 621–681.
14. Keck ZY, et al. (2009) Mutations in hepatitis C virus E2 located outside the CD81 binding sites lead to escape from broadly neutralizing antibodies but compromise virus infectivity. *J Virol* 83:6149–6160.
15. Si Y, et al. (2012) A human claudin-1-derived peptide inhibits hepatitis C virus entry. *Hepatology* 56:507–515.
16. Kong L, et al. (2013) Hepatitis C virus E2 envelope glycoprotein core structure. *Science* 342:1090–1094.
17. Sabo MC, et al. (2011) Neutralizing monoclonal antibodies against hepatitis C virus E2 protein bind discontinuous epitopes and inhibit infection at a postattachment step. *J Virol* 85:7005–7019.
18. El-Diwany R, et al. (2017) Extra-epitopic hepatitis C virus polymorphisms confer resistance to broadly neutralizing antibodies by modulating binding to scavenger receptor B1. *PLoS Pathog* 13:e1006235.
19. Guan M, et al. (2012) Three different functional microdomains in the hepatitis C virus hypervariable region 1 (HVR1) mediate entry and immune evasion. *J Biol Chem* 287: 35631–35645.

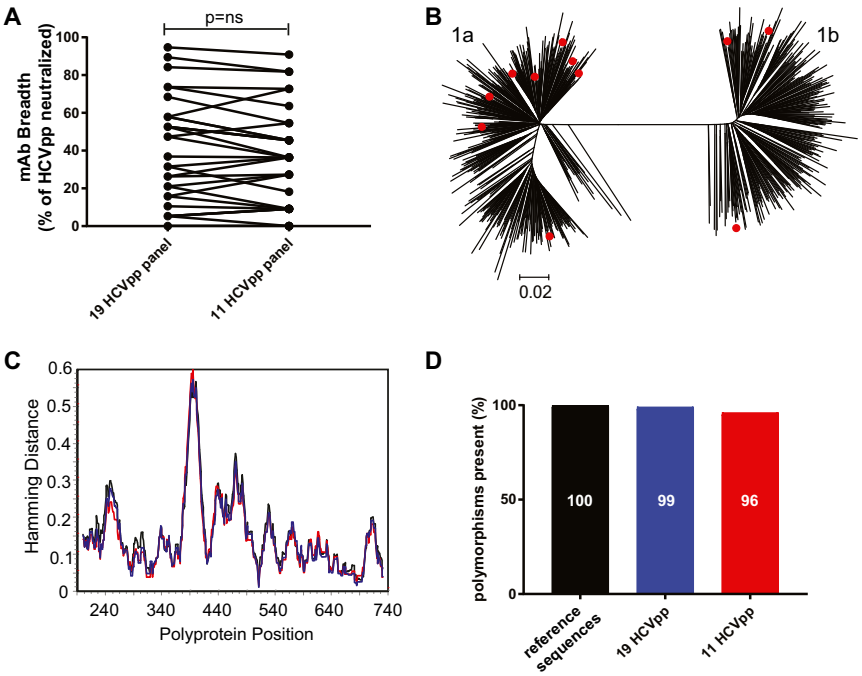

Fig. S1. Selection of a diverse and representative genotype 1 HCVpp panel. (*A*) Comparison of neutralizing breadth of 32 mAbs determined using a previously described diverse panel of 19 genotype 1 HCVpp (1, 2, 3), and the 11 HCVpp subset of that panel used in the current study. Each point indicates the neutralizing breadth of a single mAb. P = not significant (ns) by paired, two-sided t test. (*B*) Neighbor-joining tree of E1E2 amino acid sequences of 634 genotype 1a and 1b reference sequences from GenBank (4) and the 11 HCVpp used in this study (red circles), with distances computed using the JTT method. The tree is drawn to scale, with branch lengths measured in the number of substitutions per site. Evolutionary analyses were conducted in MEGA7 (5). (*C*) Diversity plot comparing variability at each E1E2 amino acid position of the reference panel of 634 genotype 1 sequences (black), the 19 HCVpp panel (blue), and the 11 HCVpp panel (red). (*D*) Percentage of amino acid polymorphisms that are present with at least 10% frequency in the 634 sequence reference set that are found in the reference sequence set (black), the 19 HCVpp panel (blue), and the 11 HCVpp panel (red).

1. Bailey JR, et al. (2017) Broadly neutralizing antibodies with few somatic mutations and hepatitis C virus clearance. *JCI Insight* 2:92872.
2. Bailey JR, et al. (2015) Naturally selected hepatitis C virus polymorphisms confer broad neutralizing antibody resistance. *J Clin Invest* 125:437–447.
3. Osburn WO, et al. (2014) Clearance of hepatitis C infection is associated with the early appearance of broad neutralizing antibody responses. *Hepatology* 59:2140–2151.
4. Munshaw S, et al. (2012) Computational reconstruction of Bole1a, a representative synthetic hepatitis C virus subtype 1a genome. *J Virol* 86:5915–5921.
5. Kumar S, Stecher G, Tamura K (2016) MEGA7: Molecular Evolutionary Genetics Analysis version 7.0 for bigger datasets. *Mol Biol Evol* 33:1870–1874.

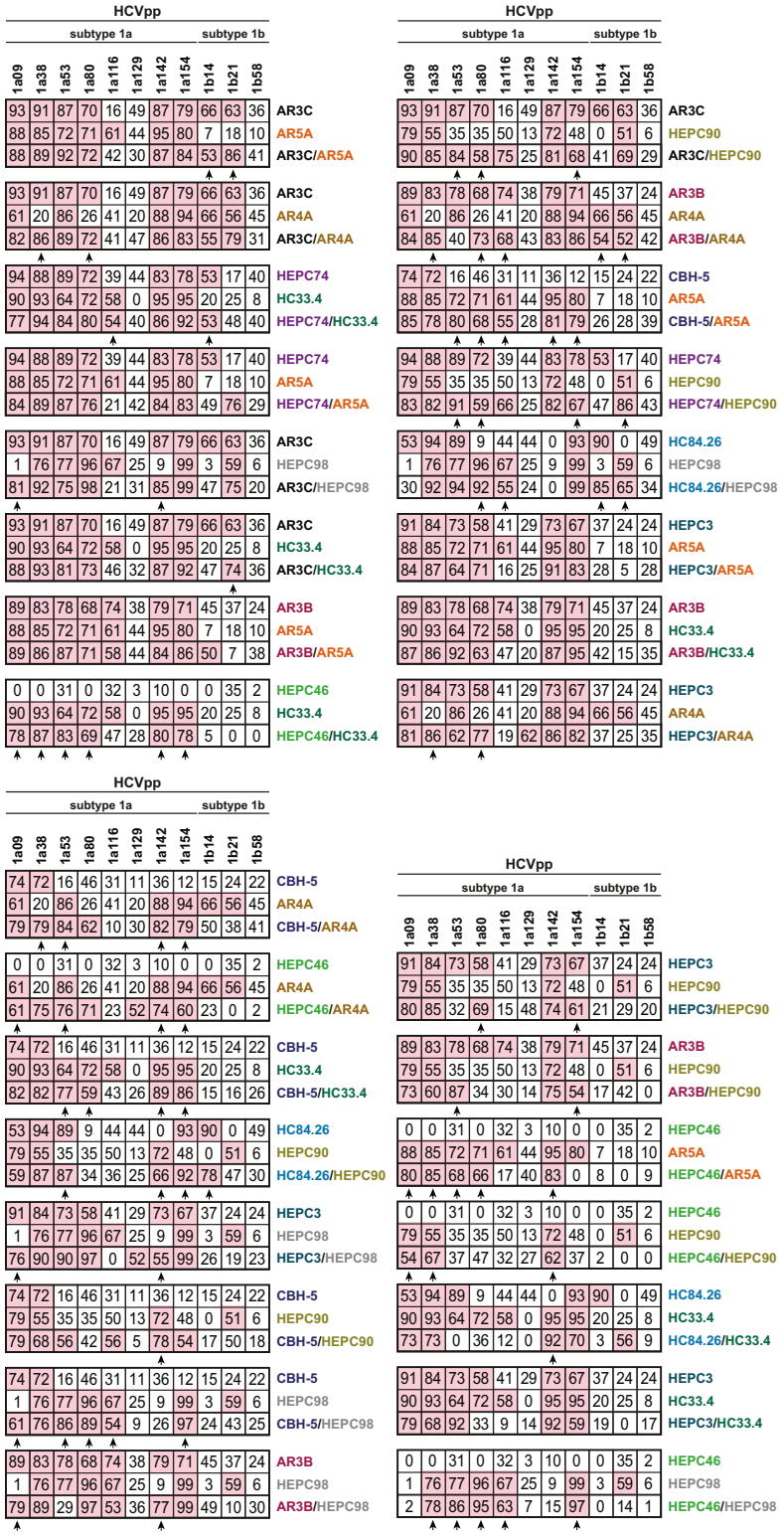

Fig. S2. Neutralization profiles of the NAb combinations not shown in Fig. 3. Values are mean percent neutralization by 10 μg/mL of each individual NAb or 10 μg/mL total concentration of NAb combinations, measured in duplicate. Pink indicates NAb/HCVpp tests with percent neutralization >50%. Arrows indicate complementary neutralization by the two NAbs in each combination.

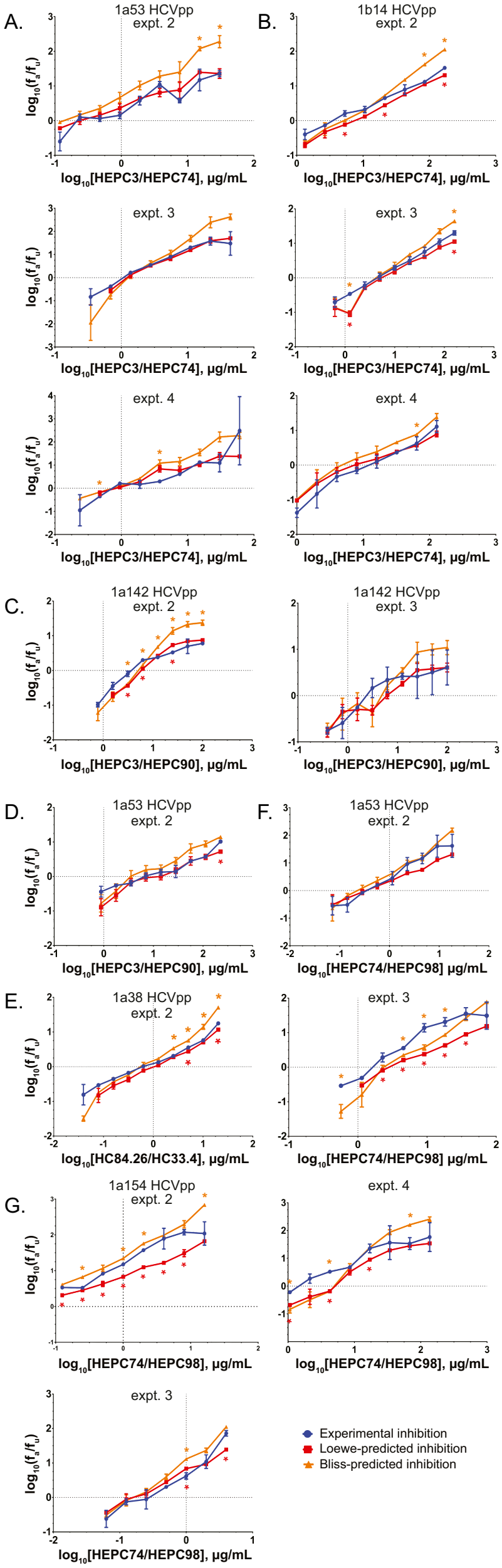

Fig. S3. Additional independent experiments assessing HEPC3/HEPC74, HEPC3/HEPC90, HC84.26/HC33.4, and HEPC74/HEPC98 neutralizing synergy, additivity, antagonism, or independence (related to Figs. 5 and 6). Each graph represents an independent experiment. Median effect plots compare experimental inhibition (blue) to the inhibition predicted by either the Loewe additivity (red) or Bliss independence (orange) models. Statistically significant differences between the experimental inhibition and Loewe or Bliss predictions are indicated with red and orange asterisks, respectively. Experimental neutralization values are the means of duplicate measurements. Loewe and Bliss values are the means of four individual predictions made at each antibody concentration using data from individual NAb neutralization, which was measured in duplicate. Error bars indicate SDs. *$P < 0.05$ by paired t tests, corrected for multiple comparisons using the Holm–Sidak method. The (*A*) 1a53 HCVpp or (*B*) 1b14 HCVpp neutralized by HEPC3/74; (*C*) 1a142 HCVpp or (*D*) 1a53 HCVpp neutralized by HEPC3/HEPC90; (*E*) 1a38 HCVpp neutralized by HC84.26/HC33.4; and (*F*) 1a53 HCVpp or (*G*) 1a154 HCVpp neutralized by HEPC74/HEPC98.

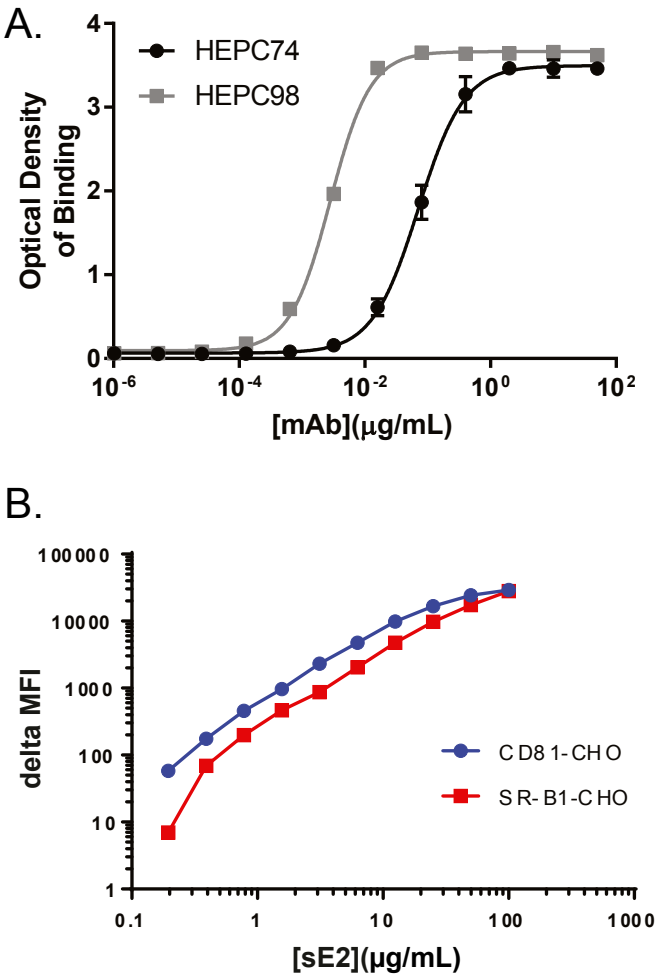

Fig. S4. Controls for sE2 binding to CD81–CHO or SR-B1–CHO cells. (*A*) ELISA binding of HEPC74 and HEPC98 to strain 1a154 sE2. (*B*) Binding of serial dilutions of 1a154 (H77) sE2 to CD81-expressing or SR-B1-expressing CHO cells. Each point was calculated from 10e4 events. Background binding to wild-type CHO cells was subtracted from MFI values.

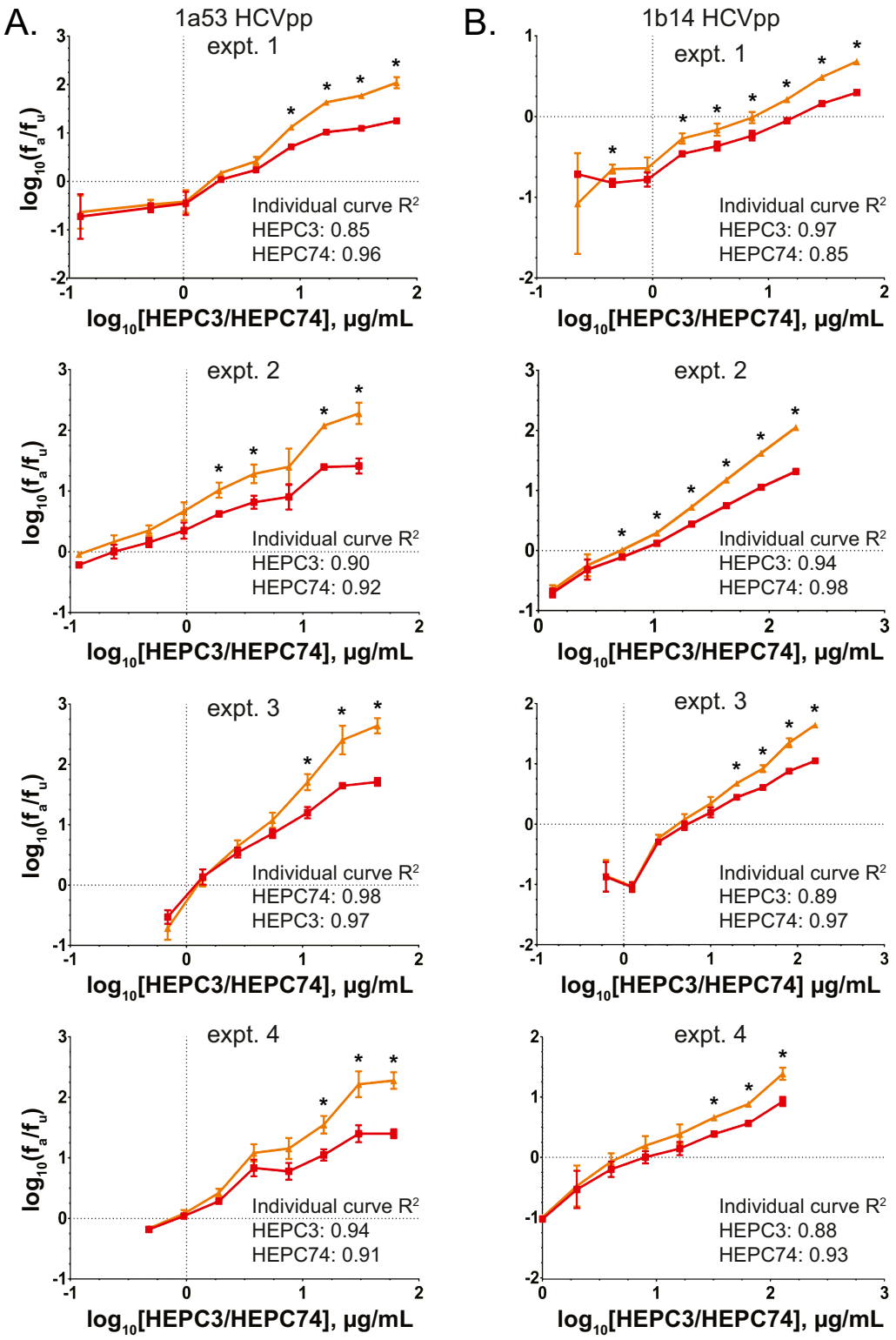

Fig. S5. (Continued)

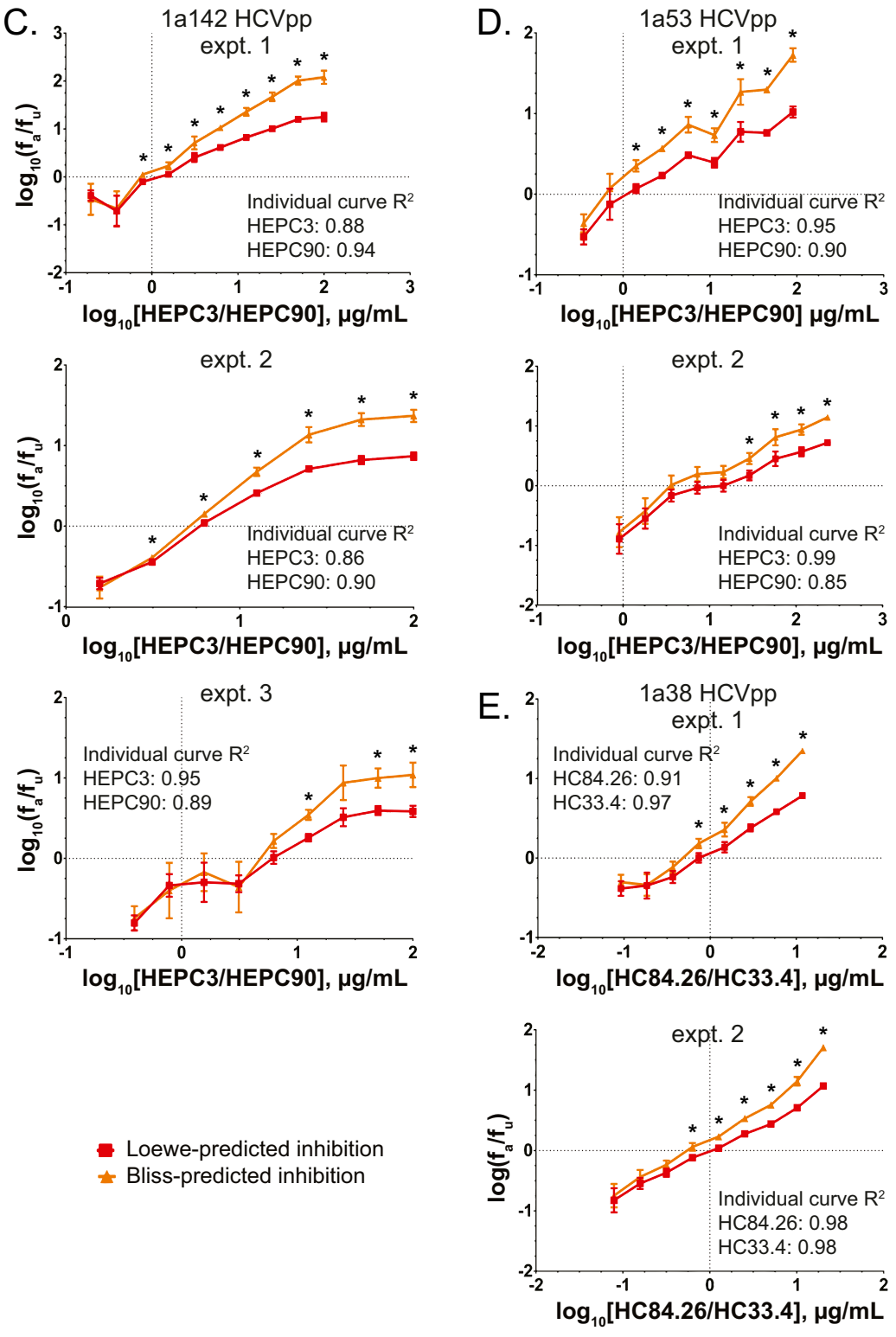

Fig. S5. (Continued)

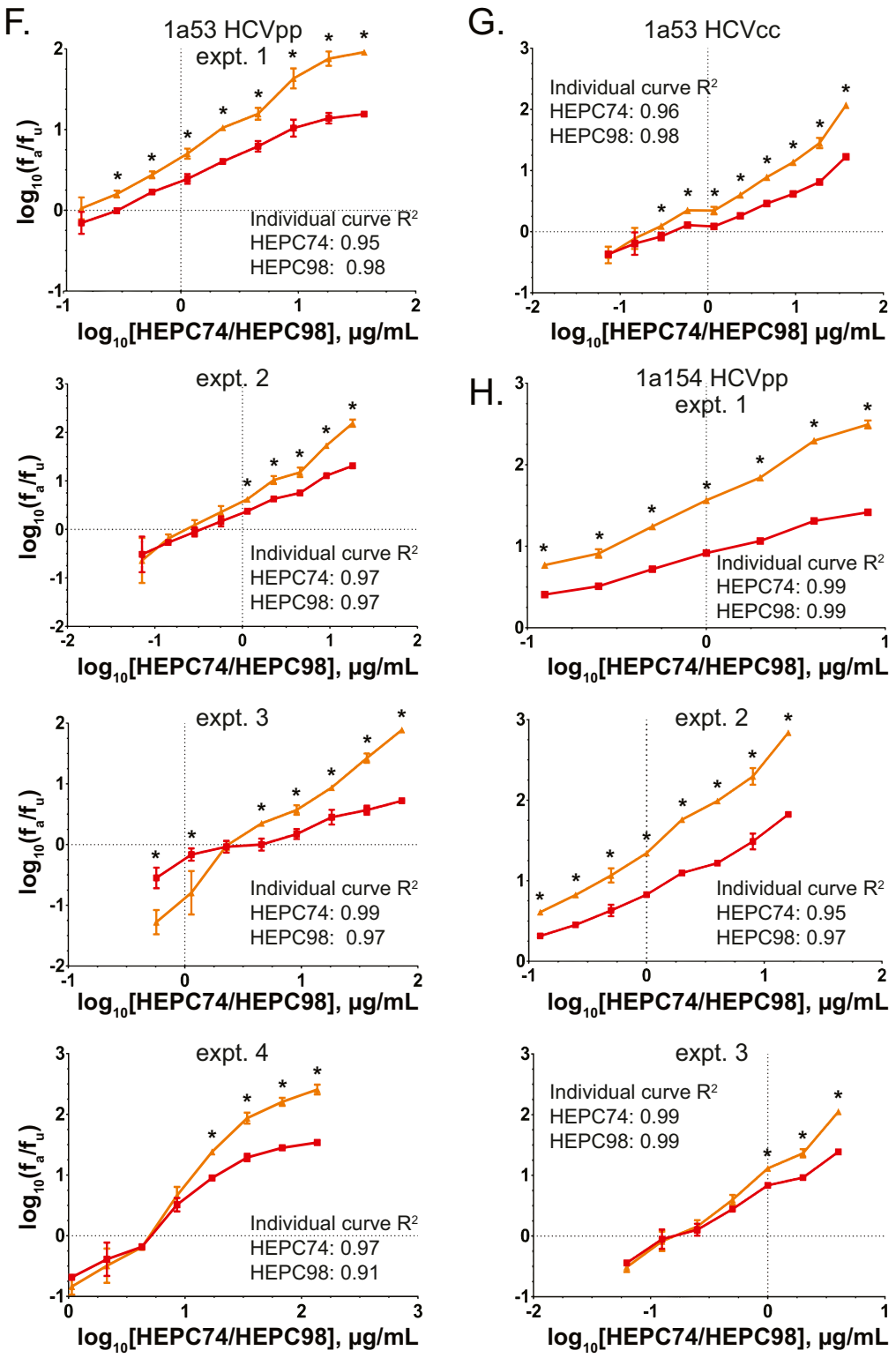

Fig. S5. Quality control for Loewe/Bliss analysis. Comparison of Loewe-predicted (red) and Bliss-predicted (orange) curves for each NAb combination experiment. Each graph represents an independent experiment. Error bars indicate SDs. To confirm that NAbs were combined in optimal ratios to allow discrimination between Loewe additivity and Bliss independence, predicted Loewe and Bliss curves for each combination were confirmed to be statistically different from each other at a minimum of three antibody concentrations. *$P < 0.05$ by paired *t* tests, corrected for multiple comparisons using the Holm–Sidak method. Values shown are *R*-squared values, calculated by linear regression, for each individual NAb neutralization curve used to calculate the Loewe and Bliss curves. Only individual NAb curves with linear relationships on median effect plots with *R* squared of >0.85 were used to calculate Loewe additivity and Bliss independence curves. (*A*) HEPC3/HEPC74, 1a53 HCVpp experiments. (*B*) HEPC3/HEPC74, 1b14 HCVpp experiments. (*C*) HEPC3/HEPC90, 1a142 HCVpp experiments. (*D*) HEPC3/HEPC90, 1a53 HCVpp experiments. (*E*) HC84.26/HC33.4, 1a38 HCVpp experiments. (*F*) HEPC74/HEPC98, 1a53 HCVpp experiments. (*G*) HEPC74/HEPC98, 1a53 HCVcc experiment. (*H*) HEPC74/HEPC98, 1a154 HCVpp experiments.

Table S1. NAbs analyzed

mAb	Antigenic domains	Critical binding residues by alanine scanning*	Refs.
CBH-5	Domain B	412, 416, 417, 418, 420, 421, 422, 423, 483, 484, 485, 488, 523, 525, 527, 530, 533, 535, 538, 540, 550	1, 2
HC84.26	Domain D	429, 441, 442, 446, 616	3
HEPC3	Antigenic region 3/domain B	425, 427, 428, 437, 499, 520, 530, 535	4
HEPC74	Antigenic region 3/domain B	425, 428, 436, 437, 530, 535	4
AR3C	Antigenic region 3/domain B	424, 488, 523, 525, 530, 535, 538, 540	5
AR3B	Antigenic region 3/domain B	412, 416, 418, 423, 424, 523, 525, 530, 535, 540	5
HEPC46	Antigenic region 1	541, 542, 543, 544, 545, 546, 548, 549, 594, 598, 633	4
HEPC98	HVR1	402, 405, 408	4
HC33.4	Epitope "1"	408, 413, 418, 420	6 7
AR5A	Antigenic region 5	201, 204, 205, 206, 639, 657, 658, 665, 692	8
AR4A	Antigenic region 4	201, 204, 205, 206, 487, 657, 658, 692, 698	8
HEPC90	NA	NA	4

NA, not available.

*Residue numbering is based on polyprotein position. Mutation of critical binding residues reported for HC84.26, HC33.4 to alanine reduce mAb binding by at least 60%. Mutation of critical binding residues reported for the remaining mAbs reduce binding by at least 50%.

1. Hadlock KG, et al. (2000) Human monoclonal antibodies that inhibit binding of hepatitis C virus E2 protein to CD81 and recognize conserved conformational epitopes. *J Virol* 74: 10407–10416.
2. Owsianka AM, et al. (2008) Broadly neutralizing human monoclonal antibodies to the hepatitis C virus E2 glycoprotein. *J Gen Virol* 89:653–659.
3. Keck ZY, et al. (2012) Human monoclonal antibodies to a novel cluster of conformational epitopes on HCV E2 with resistance to neutralization escape in a genotype 2a isolate. *PLoS Pathog* 8:e1002653.
4. Bailey JR, et al. (2017) Broadly neutralizing antibodies with few somatic mutations and hepatitis C virus clearance. *JCI Insight* 2:92872.
5. Law M, et al. (2008) Broadly neutralizing antibodies protect against hepatitis C virus quasispecies challenge. *Nat Med* 14:25–27.
6. Keck Z, et al. (2013) Cooperativity in virus neutralization by human monoclonal antibodies to two adjacent regions located at the amino terminus of hepatitis C virus E2 glycoprotein. *J Virol* 87:37–51.
7. Keck ZY, et al. (2016) Antibody response to hypervariable region 1 interferes with broadly neutralizing antibodies to hepatitis C virus. *J Virol* 90:3112–3122.
8. Giang E, et al. (2012) Human broadly neutralizing antibodies to the envelope glycoprotein complex of hepatitis C virus. *Proc Natl Acad Sci USA* 109:6205–6210.